Electrolytic Membrane Recovery of Bromine from Waste Hydrogen Bromide Streams

Cary N. Wauters and Jack Winnick
School of Chemical Engineering, Georgia Institute of Technology, Atlanta, GA 30332

A novel electrochemical process was developed for the recovery of bromine from waste gas-phase hydrogen bromide streams. It uses a molten-salt-saturated membrane to electrolytically decompose hydrogen bromide into its molecular constituents, which are separated into a hydrogen-enriched waste stream and a pure bromine product stream. Single-cell studies were carried out in a configuration consisting of two cell housings (vitreous carbon), two gas-diffusion electrodes (reticulated vitreous carbon or graphite felt), and a molten salt [$(Li_{0.575}K_{0.133}Cs_{0.292})Br$] saturated membrane (zirconia). Single-cell results at 300°C, based on process stream concentrations ranging from 25 to 75% hydrogen bromide at 50 to 300 mL/min, demonstrated current densities exceeding 1 A/cm^2 and removals as high as 95%. Water and acetone (as a light organic contaminant) addition to the process feed, as well as exposure to thermal cycling, showed no deleterious effects on cell performance. Preliminary economics indicate this to be a viable process.

Introduction

A novel electrochemical process can be used for the recovery of bromine (Br_2) from waste gas-phase hydrogen bromide (HBr) streams (Winnick, 1997). The process involves the use of a molten-salt-saturated membrane to electrolyze HBr; the molecular constituents are then separated into a hydrogen (H_2) enriched process stream and a Br_2 product stream.

The demand for a Br_2 recovery process stems from the increasingly stringent economic and environmental constraints associated with the production of brominated organic compounds (primarily flame retardant and agricultural chemicals). These products demand nearly 65% of the approximately 400,000,000 kg of Br_2 produced annually (Lyday, 1994). However, 50% of the Br_2 used results in the generation of byproduct HBr (typically gas-phase) or a potential for recycle of approximately 130,000,000 kg Br_2 annually.

In addition to the aforementioned industrial interest in Br_2 recovery, the growth of the H_2 industry has also prompted the development of several aqueous-based HBr electrolysis processes (Schuetz and Fiebelmann, 1974; Kondo et al., 1983). Some later versions were refined to incorporate proton exchange membranes (PEMs). The major drawback, however, was the production of Br_2 within the process stream, thus requiring further separation steps. In addition, the aqueous environments required the careful maintenance of the water/electrolyte balance as well as exotic electrode materials.

More recently, a catalytic method for producing Br_2 from HBr has been developed. The technology, however, is inherently complex and unit-operation intensive (Anonymous, 1992).

Theory

Traditional membrane gas-phase separations rely upon a chemical potential difference ($\Delta\mu_i$) as the driving force

$$\Delta\mu = \mu_i - \mu_i' = RT\ln\left(\frac{a_i}{a_i'}\right) \tag{1}$$

where R denotes the gas constant, T is the absolute temperature, a_i is the activity with respect to species i, and the prime is the extractive phase. Typically, a pressure or concentration difference provides the driving force.

Correspondence concerning this article should be addressed to C. N. Wauters at his current address: Merck & Co., Inc., P.O. Box 7, Elkton, VA 22827.

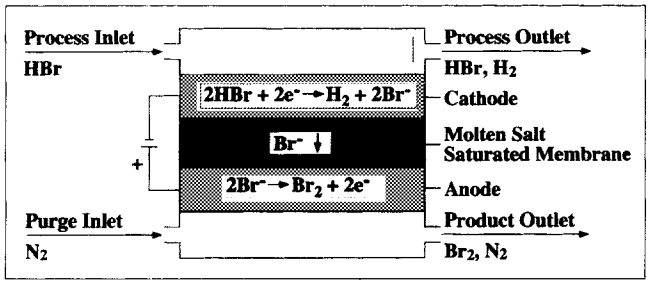

Figure 1. Bromine recovery process.

However, in special circumstances, when dealing with a charged species or charged intermediate species, an electrochemical difference ($\Delta\bar{\mu}_i$) can instead be used

$$\Delta\bar{\mu} = \bar{\mu}_i - \bar{\mu}'_i = \mathrm{RT}\ln\left(\frac{a_i}{a'_i}\right) + z_i F\Delta\Phi \tag{2}$$

where z_i denotes the charge with respect to species i and F is the Faraday constant. In this case, an electric potential difference ($\Delta\Phi$) provides the driving force (Winnick, 1990).

With regard to Br_2 recovery (Figure 1), a process stream is introduced to the cathode where the HBr is reduced

$$2\mathrm{HBr} + 2\mathrm{e}^- \rightarrow \mathrm{H}_2 + 2\mathrm{Br}^- \tag{3}$$

The reaction results in the production of gas-phase H_2 and bromide anions (Br^-). While a molten-salt saturated membrane configured between the cathode and anode isolates the H_2 to the process stream, the Br^-s are allowed to migrate via the potential difference described earlier in Eq. 2 to the anode where they are oxidized

$$2\mathrm{Br}^- \rightarrow \mathrm{Br}_2 + 2\mathrm{e}^- \tag{4}$$

The operation thus yields a separate Br_2 product stream.

At equilibrium, the potential required to carry out HBr electrolysis is described by the Nernst relation (Walsh, 1993)

$$E_e = E^o + \frac{\mathrm{RT}}{nF}\ln\left(\frac{[\mathrm{HBr}]_{\mathrm{C}}^2}{[\mathrm{H}_2]_{\mathrm{C}}[\mathrm{Br}_2]_{\mathrm{A}}}\right) \tag{5}$$

where E^o denotes the standard potential of approximately -0.6 V, a value substantially less than that of possible parasitic reactions involving common industrial contaminants such as water and light organic compounds. n denotes the number of electrons transferred (2).

To carry out exhaustive electrolysis of the entering HBr, the stoichiometric current density (i_{stc}), is defined by

$$i_{\mathrm{stc}} = \frac{x\dot{v}nF\dfrac{P}{\mathrm{RT}}}{A} \tag{6}$$

where x denotes the entering mol fraction of HBr, $\dot{v}$ is the volumetric flow rate, P is the pressure, and A is the electrode area (in this instance, the superficial electrode area, since porous electrodes were employed).

Experimental Studies

The single-cell apparatus underwent a series of modifications aimed at enhancing cell performance (Wauters and Winnick, 1996). However, the core configuration remained the same consisting of five salient components: two cell housings, two gas-diffusion electrodes, and a molten-salt-saturated membrane (Figure 2). Depending upon the modification, the superficial electroactive area ranged from 7.9 to 15.5 cm^2.

The cell housings served to direct the flow of the products, reactants, and current to the respective electrodes. The parts were machined from a high density graphite stock. The cell housings were then vitrified to prevent the loss of electrolyte (Electrosynthesis Co., Lancaster, NY), an effect observed in preliminary trials using standard high density graphite due to its microporous structure.

Gas diffusion electrodes were utilized to maximize the electroactive gas/electrode/electrolyte interfaces. They were fashioned from either reticulated vitreous carbon or graphite felt (Electrosynthesis Co.).

Zirconia (8% yttria stabilized) membranes (Zircar) were used to entrain a molten salt electrolyte. To minimize the operating temperature, a ternary eutectic mixture ($Li_{0.575}K_{0.133}Cs_{0.292}$)Br (Sigma) with a melting point of approximately 250°C was selected.

The process (cathode) inlets included three predefined mixtures: (1) 25%, (2) 50%, and (3) 75% HBr, balance nitrogen (N_2) (Matheson and Air Products). The process flow rates ranged from 50 to 300 mL/min and were controlled using a specialized flowmeter assembled using Kynar, Viton, and Teflon parts with tantalum and sapphire floats (Brooks). The process pressure was maintained at approximately 15 psig (103 kPa) using a two-stage stainless steel regulator (Matheson). In specific cases, industrial conditions were more closely mimicked through the introduction of water and acetone (as a light organic contaminant) by sparging the process stream through a 48% hydrobromic acid or a 48% hydrobromic acid and acetone solution (Sigma) via a standard glass bubbler prior to introduction to the cell.

High purity N_2 (Air Products) was provided as the product (anode) purge and was maintained at 100 mL/min using a standard flowmeter (Air Products) and approximately 15 psig using a standard single-stage regulator (Air Products). The

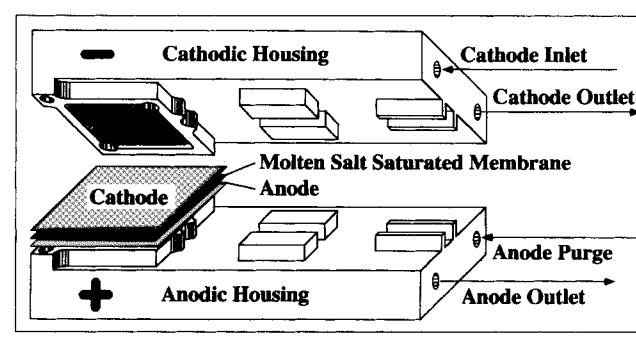

Figure 2. Single-cell configuration.

process inlet and outlet as well as product outlet lines were Teflon with Kynar unions.

HBr removal was measured by analyzing the process outlet concentrations using Fourier transform infrared spectroscopy (FTIR) (Perkin Elmer Paragon 500) with a 10-cm path glass cell and calcium fluoride (CaF_2) windows. Periodically, the anode outlet concentrations were also monitored to check for HBr crossover or molecular recombination. The system was calibrated using the predefined HBr mixtures described earlier. The FTIR cell and all lines between the FTIR and furnace were maintained at approximately 85°C using heating tape (Fisher) to prevent condensation.

Initially a membrane (~ 1 mm thick) was saturated in a molten-salt electrolyte bath, removed, and rapidly cooled. The membrane was then quickly arranged within the cell and the assembly transferred to a modified Lindberg Furnace. To aid in membrane transfer, the electrodes were tacked in place using small tabs of cellophane tape. Further, a single layer of borosilicate glass fiber fabric (Fisher) was tacked over the susceptible exposed regions of the housings to avoid short circuiting. The cell was ramped to the operating temperature of 300°C at 1°C/min. Once the 300°C operating temperature was achieved, a 1-kg weight was added to the top of the assembly to aid in maintaining gas-tight seals.

During startup, high purity N_2 was used to purge both the cathode and anode. To assure that the configuration had achieved gas-tight wet seals, the outlet flow rates were monitored using a bubble meter (Ace Glass) and compared with the inlet flowmeter-controlled values.

Standard battery clip leads (Ack) were used to connect cell housings to a Hewlett Packard 6274 DC power supply; the cell was operated under galvanostatic conditions. Currents and potentials were monitored using Fluke 8012A and Simpson Model 460 Series 4 multimeters. A Techtronix oscilloscope was used to monitor ohmic resistance using the standard current-interrupt technique (Bauer, 1972).

At trial termination, the cell was typically disassembled hot to remove the membrane intact for postmortem analysis.

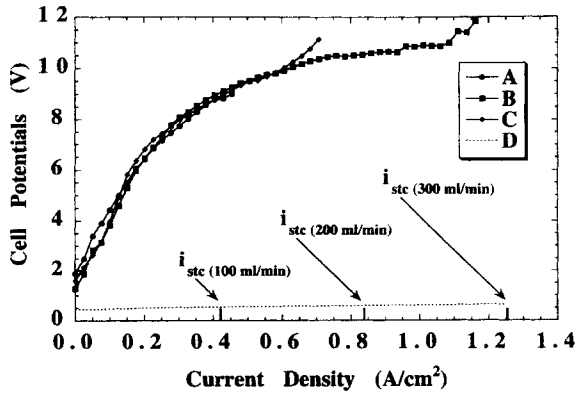

Figure 3. Potentials with applied current density and varying process (cathode) flow rate using a process inlet of 50% HBr, balance N_2, and product (anode) purge of N_2 at 100 mL/min.

(A) Experimental 100 mL/min; (B) experimental 200 mL/min; (C) experimental 300 mL/min; (D) calculated equilibrium (experimental values are uncompensated).

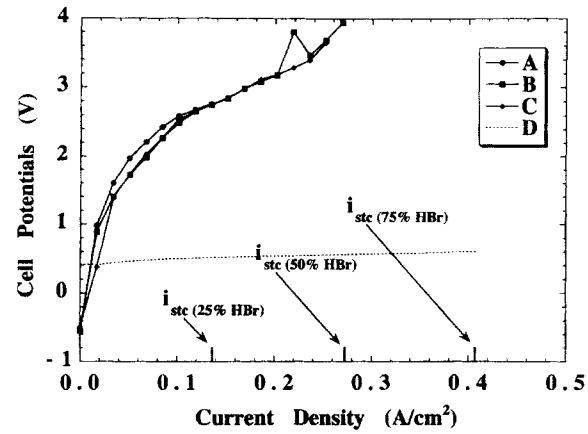

Figure 4. Potentials with applied current density and varying process (cathode) concentration using a process inlet at 100 mL/min and a product (anode) purge of N_2 at 100 mL/min.

(A) Experimental 25% HBr, balance N_2; (B) experimental 50% HBr, balance N_2; (C) experimental 75% HBr, balance N_2; (D) calculated equilibrium (experimental values are uncompensated).

Results and Discussion

Cell voltages are shown in Figure 3 for a variety of process flow rates. The calculated equilibrium potentials (Eq. 5) and stoichiometric current densities (Eq. 6) are shown as well. Due to the high levels of HBr, no variation with the flow rate was observed. An unexpected characteristic common to the trial results was the high magnitude of the cell potentials. This issue will be addressed later in the discussion.

It was further observed that the cell potentials associated with a varying process (HBr) inlet concentration also remained approximately equivalent (Figure 4). This behavior was again attributed to the relatively high concentrations of HBr introduced as the process (cathode) inlet.

While the precise cause for the high cell potentials remains unknown, the effect is likely the result of some interfacial phenomena. Possible factors include: uneven contact between the electrodes and housings, shifts in the electrode/electrolyte interfaces, and/or bubble formation (H_2 or Br_2). Indeed, the last factor is supported by a notable ohmic resistance dependence on current density (Figure 5). These ohmic resistances, however, are not nearly accounted for when compared with calculations based on cell geometry using manufacturer and literature resistivities (approximately 1.0×10^{-2} Ω or less).

Activation overpotentials were presumed to be negligible due to the use of a molten salt and the relatively high operating temperature of the system. Concentration overpotentials were, likewise, thought to be modest due, again, to the high HBr inlet concentrations.

Despite the higher than expected cell potentials, outstanding HBr removals were obtained (Figure 6). The results accurately reflect stoichiometric calculations (suggesting nearly 100% current efficiency). Further, removals exceeding 95% were obtained. This is impressive considering the gas residence time is less than 1 s. Product Br_2 was found to be more than 99+% pure (detected water and trace organic com-

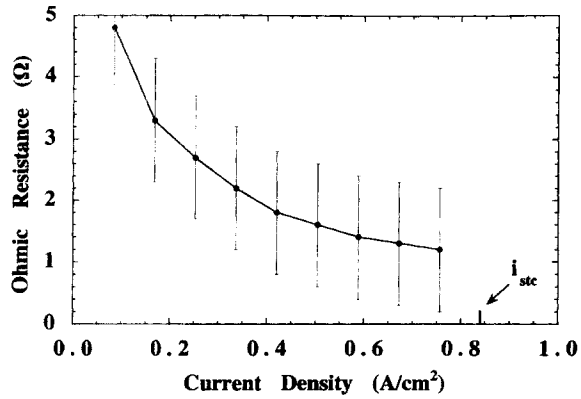

Figure 5. Ohmic resistance with applied current density using a process (cathode) inlet of 25% HBr (balance N_2) at 200 mL/min and product (anode) purge of N_2 at 100 mL/min.

pounds, not present in the feed, were attributed to collection).

To more closely mimic industrial conditions, both water vapor (~ 1%), as well as water vapor and acetone (as a qualitative measure), were introduced to the process inlet. The polarization data remained essentially unchanged (Figure 7). The approximate 2 V spread in the data is attributed to the shifts in the electrode/electrolyte interfaces, which occurred over the extended time period over which data were taken.

The cell was also subjected to thermal cycling. Following several hours of operation, the cell was allowed to cool overnight (under N_2) and reinitiated approximately 12 h later. Polarization data reflected minor variation, demonstrating the robust nature of the cell (Figure 8). Deviations were again attributed to shifts in the electrode/electrolyte interface over the extended time period. This was unexpected as typical molten-salt-saturated membrane systems are particularly susceptible to thermal damage.

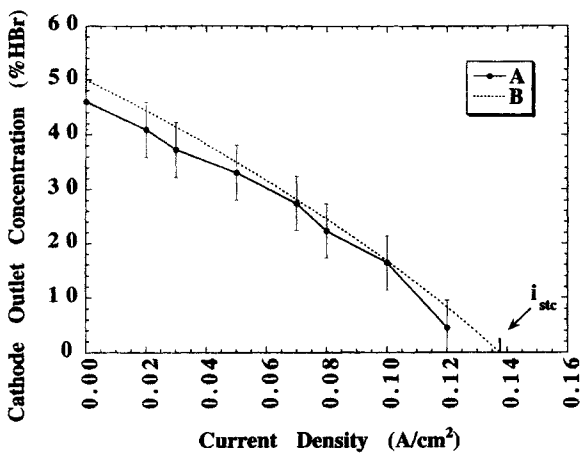

Figure 6. Process (cathode) outlet concentration with applied current density using a process inlet of 50% HBr (balance N_2) at 50 mL/min and product (anode) purge of N_2 at 100 mL/min.

(A) Experimental; (B) calculated.

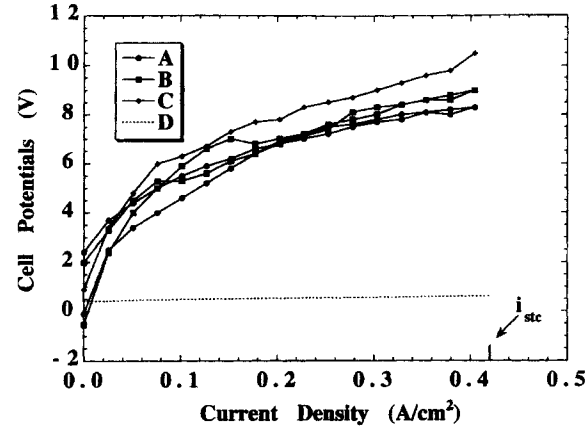

Figure 7. Potentials with applied current density using a process (cathode) inlet at 100 mL/min and a product (anode) purge of N_2 at 100 mL/min.

(A) Experimental 50% HBr, balance N_2; (B) experimental 50% HBr with water vapor, balance N_2; (C) experimental 50% HBr with water vapor and acetone, balance N_2; (D) calculated equilibrium (experimental values are uncompensated).

Economics

The scale-up of the Br_2 recovery process is projected to follow that of the molten carbonate fuel cell (MCFC) adopting the bipolar array configuration (Figure 9). Operating costs, calculated by

$$C_{op} = \frac{C_{elec} E_{cell} Fn}{MW_{Br_2}} \tag{7}$$

where C_{elec} denotes the cost of electricity at \$0.03/kWh, E_{cell} is the cell voltage, and MW_{Br_2} is the molecular weight of Br_2, predict approximately \$0.10/kg of Br_2 produced (based

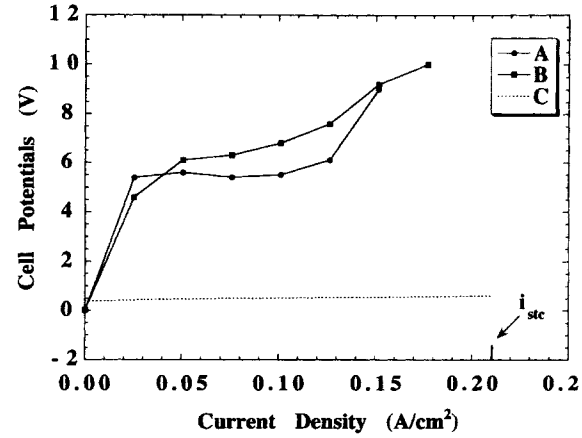

Figure 8. Thermally cycled potentials with applied current density using a process (cathode) inlet of 50% HBr (balance N_2) at 50 mL/min and product (anode) purge of N_2 at 100 mL/min.

(A) Experimental cycle I, (B) experimental cycle II, and (C) calculated equilibrium (experimental values are uncompensated).

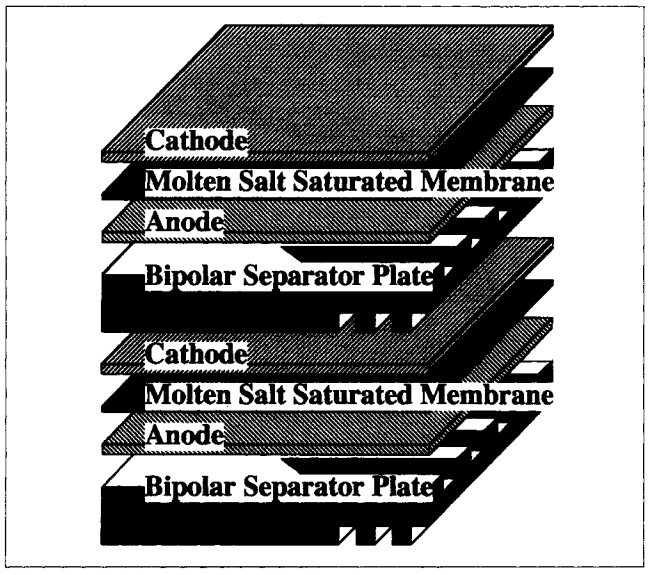

Figure 9. Bipolar array.

roughly on experimental 10 V cross cell potentials). However, with further development, 1 V cross cell potentials are more realistic, suggesting an operating cost of only about \$0.01/kg of Br_2 produced. The current market value of high quality Br_2 is approximately \$1.10/kg.

To estimate the capital cost of a reasonably sized facility, the costs of a MCFC plant requiring the same active electrode area were used (Appleby and Foulkes, 1989; Wauters, 1997). This seems to be a conservative method, because the configuration of the two are the same (a bipolar array) yet the material costs for the MCFC should be higher using nickel electrodes rather than carbon as used here. Furthermore, the temperature of operation of the MCFC is 650°C, some 350°C higher than the bromine recovery process.

On this basis, a plant was sized for an HBr process stream of 1,320,000 kg/yr operating at 90% removal efficiency (equivalent to 1,170,000 kg Br_2/yr, roughly 1% of the global production of the byproduct HBr). To achieve this goal, the process would require an active surface area of approximately 9 m^2, which is that needed for a 12 kW MCFC. The area was fixed using an operating current density of 0.5 A/cm^2, well within the limits of the laboratory study. The installed cost of the facility is estimated at about \$100,000, which may be amortized within the first year as shown in Table 1.

Table 1. First-Year Profit Based on Process Feed of 1,320,000 kg of Byproduct HBr/yr (1,170,000 kg Br_2/yr at 90% Removal) and Operation at 0.5 A/cm^2

Capital Cost (\$)	Operating Cost (\$/yr)	Bromine Produced (\$/yr)	Profit (First Yr)
Based on 1 V:			
−100,000	−11,700	1,287,000	1,175,000
Based on 10 V:			
−100,000	−117,000	1,287,000	1,070,000

Conclusion

A novel electrochemical process for the recovery of Br_2 from waste gas-phase HBr streams has been developed. Single-cell studies have demonstrated the industrial viability of such a process. Despite higher than expected cell potentials, single-cell studies (based on process stream concentrations ranging from 25 to 75% HBr at 50 to 300 mL/min) have demonstrated current densities which exceed 1 A/cm^2 and removals as high as 95%. The addition of water and acetone, as well as subjection to thermal cycling, performed to more closely mimic industrial conditions, have shown no significant decline in cell performance. Work is continuing which is aimed at reducing the high cell voltages.

Acknowledgment

The authors wish to express their sincere appreciation to the Albemarle Corporation (in particular, Ronald Camp, Robert Davis, and Phillip Beaver) for the financial support of this project, POCO Graphite Inc. for the donation of graphite materials, and to L. Andra Wauters for her assistance and support.

Literature Cited

Anonymous, "New Oxidation Process Extracts Bromine," *Chem. Eng. Prog.*, **88**, 16 (1992).

Appleby, A. J., and F. R. Foulkes, *Fuel Cell Handbook*, Van Nostrand Reinhold, New York (1989).

Bauer, H., *Electrodics*, Thieme, New York (1972).

Kondo, W., S. Mizuta, Y. Oosaw, T. Kumagai, and K. Fujii, "Decomposition of Hydrogen Bromide and Iodide by Gas Phase Electrolysis," *Bull. Chem. Soc. Jpn.*, **56**, 2501 (1983).

Lyday, P. A., *Mineral Industry Surveys*, U.S. Bureau of Mines, Washington, DC (1994).

Schuetz, G. H., and P. J. Fiebelmann, Luxembourg Patent No. 71,037 (1974).

Walsh, F. C., *A First Course in Electrochemical Engineering*, The Electrochemical Consultancy, Hants, England (1993).

Wauters, C. N., "Electrolytic Membrane Recovery of Bromine from Waste Gas-Phase Hydrogen Bromide Streams Using a Molten Salt Electrolyte," PhD Thesis, Georgia Inst. of Technology (1997).

Wauters, C. N., and J. Winnick, "Recovery of Bromine from Waste Gas-Phase Hydrogen Bromide Streams Using an Electrolytic Membrane," *J. Electrochem. Soc.*, **143**, L184 (1996).

Winnick, J., "Electrochemical Membrane Gas Separation," *Chem. Eng. Prog.*, **86**, 41 (1990).

Winnick, J., U.S. Patent No. 5,618,405 (1997).

Manuscript received May 11, 1998, and revision received Aug. 20, 1998.